COBEM 2023 27TH INTERNATIONAL CONGRESS OF MECHANICAL ENGENEERING

ABCM Brazilian Society of Mechanical Sciences and Engineering
27th ABCM International Congress of Mechanical Engineering
December 04-08, 2023, Florianópolis-SC, Brazil

COB-2023-1638
MORPHOLOGICAL PROPERTIES EVALUATION OF POROUS AND ANISOTROPIC MATERIALS

Lívia Mendonça Nogueira
Universidade Federal do Rio de Janeiro (UFRJ)
Centro de Educação Tecnológica Celso Suckow da Fonseca (CEFET/RJ)
livia.nogueira@cefet-rj.br

Lavinia Maria Sanabio Alves Borges
Universidade Federal do Rio de Janeiro (UFRJ)
lavinia@mecanica.coppe.ufrj.br

Daniel Alves Castello
Universidade Federal do Rio de Janeiro (UFRJ)
dnl.castello@gmail.com

Abstract. *In the context of the mechanical behavior of materials, predicting the safe limits for a material under a general state of stress requires the application of failure criteria. There are well-established failure criteria for isotropic materials like Mises, Tresca, and Mohr-Coulomb. Nonetheless, materials that exhibit porous and microstructural anisotropy are still challenging, especially concerning the morphology–elasticity relationships. This is a particularly important issue in cellular materials (like bones) and geological materials (like rocks), in which the ability to predict safe load conditions is fundamental in applications such as osteoporosis diagnosis in the medical field, and drilling efficiency in the oil and gas industry. The main goal of this work is to evaluate the use of the Mean Intercept Length (MIL) method to construct fabric tensors that could characterize morphological properties of porous and anisotropic materials. The methodology is based on micromechanical modeling that aim to develop an equivalent continuum that properly models the heterogeneous material, based on the geometry and properties of the individual phases. Regarding the geometric characterization of the microstructure of porous materials, although the volume fraction (or porosity) is recognized as the main parameter of the material's heterogeneity, it does not provide information about the orientation of the microstructure. Within the elasticity context, the approach used to model the microstructure architecture consists of introducing higher-ranking tensors, called fabric tensors. ImageJ software was used for benchmark image analysis in which fabric tensors are estimated using the MIL method. The results showed good agreement with those expected as a homogenization procedure and opened the perspective of using this tool in elasticity models and failure criteria for anisotropic porous materials.*

Keywords: *microstructure, elasticity, porous, anisotropy, fabric tensors*

1. INTRODUCTION

Material failure is generally defined in terms of load-carrying or energy storage capacity when material either yields or fractures. A material under uniaxial loading can have its failure experimentally determined by a uniaxial tensile test. Nonetheless, in actual service, most materials are subjected to a variety of loading conditions (e.g., biaxial or triaxial stresses), and establishing failure conditions by experimental methods becomes unfeasible, or at least inconvenient. Therefore, it is essential to set failure criteria based on material properties and conditions such as temperature or loading rate for predicting the material safe limits under a general stress state (Chakrabarty, 2012; Hill, 1998).

For isotropic materials such as metals and ceramics, there are well-established failure criteria like those given by von Mises, Tresca, and Mohr-Coulomb. However, when the material is porous (heterogeneous) and its mechanical properties are orientation-dependent (anisotropic), both the failure mechanism establishment and the way such material characteristics influence its material behavior are still challenging (Gao et al., 2010; Pietruszczak et al. 2001; Keralavarma et al., 2016).

Although it is frequently assumed that materials are isotropic, they rarely are. There are two leading causes of anisotropy: one cause is the preferred orientations of grains or crystallographic texture; the second one is mechanical fibering, which is the elongation and alignment of microstructural features, such as inclusions and grain boundaries (Hosford, 2010). Natural materials like wood, rock, and biological tissues, as well as synthetic fiber-reinforced composites, exhibit this microstructure feature at a significant level. Besides that, voids in heterogeneous materials also influence the elastic properties and the failure mechanism.

This work aims to evaluate and quantify relevant morphological parameters for microstructural characterization to be incorporated in elasticity relationships and failure criteria for anisotropic porous materials.

2. MICROMECHANICAL MODELING

Material heterogeneity occurs at many different length scales. Regarding the use of continuum models, heterogeneity scales should normally be at least an order or two smaller than the behaviors sought. Based on this, these heterogeneous features are normally referred to as microstructure (Sadd, 2018).

One of the fundamental goals of micromechanical material modeling is to develop theories to predict the response of heterogeneous materials based on the geometries and properties of the individual phases. In this sense, the effort is to develop an equivalent continuum that properly models the heterogeneous material.

Analytical studies have recently constructed various generalizations of classical continuum theories by introducing different micro-behaviors into the basic theory. The volume fraction (or porosity) is considered the primary parameter in the geometric characterization of the microstructure of porous or granular materials. However, as a scalar quantity, it does not provide any information about the arrangement of the microstructure. In this regard, it is necessary to introduce additional parameters able to describe such orientations. Within the elasticity context, the approach commonly used to model the microstructure architecture involves introducing higher-ranking fabric tensors (Skrzypek & Ganczarski, 2015).

2.1 Fabric tensors

The term fabric is often used to describe geometry discontinuities or internal microstructural packing geometry of granular materials. Observations indicate that granular microstructure produces well-defined loading chains that transfer most forces through the material (Sadd, 2018). In modern scientific literature, the concept of fabric tensor is widely used to describe the structural features of various materials. Although it initially emerged in the geological field to describe the structure of geological media (Pietruszczak & Pakdel, 2022; Singh et al., 2022, Hu et al., 2021, Badakhshan et al., 2021, Lydzba et al., 2003), this approach has been spread to other research areas. In medicine, it is applied to study the structure of bone tissue (Lekadir et al., 2016; Moreno et al., 2016; Charlebois et al., 2010; Kreipke & Niebur, 2017) and in materials science, it is commonly used for composites and damage applications (Voyiadjis & Kattan, 1999; De Pascalis et al, 2022; Voyiadjis et al., 2007; Jeppesen et al, 2021).

Briefly, fabric tensors are understood as symmetric second-rank tensors that characterize a material's structural sensitivity. The concept lies in modeling the material microstructure through tensors of higher rank orders which characterize both anisotropy and orientation. These tensors are semi-global measurements since they are computed in relatively large neighborhoods, which are assumed quasi-homogeneous (Smolin et al., 2019).

In order to relate fabric tensors to the material's mechanical properties, Cowin (1985) firstly assumed that the material base of the porous elastic solid is isotropic, and the fabric tensor completely determines the anisotropy. He developed an explicit algebraic relationship based on a polynomial function between the fourth-rank elasticity tensor and the fabric tensor of a porous, anisotropic, and linear elastic material. Besides that, it was also shown that the material symmetries of orthotropy, transverse isotropy, and isotropy correspond to the cases of three, two, and one distinct eigenvalues of the fabric tensor, respectively.

Among the methods proposed in the literature to calculate fabric tensors, the Mean Intercept Length (MIL) is considered in this work thanks to the large amount of evidence supporting its appropriateness to predict mechanical properties in oriented materials (Moreno et al., 2014; Ketcham, 2005; Kahl et al., 2017).

2.2 Mean Intercept Length (MIL)

The Mean Intercept Length (MIL) approach has been proposed to construct the fabric tensor for biphasic materials. The concept is based on defining the mean distance between a change from one phase to another along a specific orientation. Whitehouse (1974) and Underwood (1973) first introduced the traditional methodology for computing the Mean Intercept Length based on the directed secants method summarized next.

From planar image sections through a polished specimen of material, an array of parallel lines to a specified direction are traced, and the number of intersections between these lines and the interface between both phases is counted, as can be schematically seen in Figure 1.

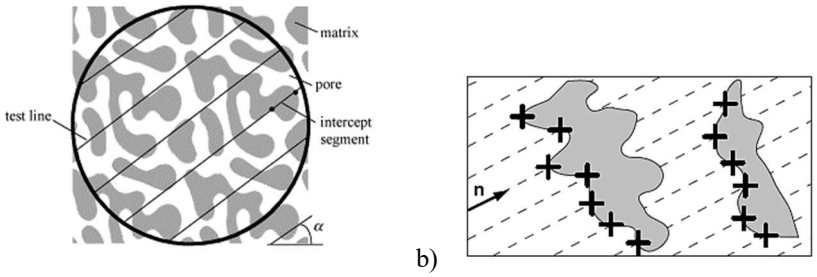

a) b)

Figure 1. Procedures for calculating the MIL: a) an array of parallel lines is traced in α direction for a binary image; b) the number of intercepts between the set of parallel lines and the interface between phases is counted. (Adapted from Chiang et al. (2006), Moreno et al. (2011)).

The Mean Intercept Length of a specific orientation, characterized by a unit vector $\boldsymbol{n}$, is a scalar quantity calculated as follows:

$$MIL(\boldsymbol{n}) = \frac{\ell}{C(\boldsymbol{n})} \tag{1}$$

where ℓ is the total length of traced lines, and $C(\boldsymbol{n})$ is the number of boundary hits in the direction specified by vector $\boldsymbol{n}$.

In partially oriented microstructures, Underwood (1973) and Whitehouse (1974) observed that when MIL data was disposed on a polar plot and fitted into an ellipse, the corresponding ellipse parameters could be correlated to the material orientation. Based on this evidence, Harrigan & Mann (1988) observed that in 3D cases, the Mean Intercept Length would similarly be represented by ellipsoids. The quadratic form for the ellipsoid generated in the polar diagram of the MIL is then established as:

$$\boldsymbol{x}^T \boldsymbol{A} \boldsymbol{x} = 1 \tag{2}$$

where $\boldsymbol{x}$ corresponds to the coordinate vector, and $\boldsymbol{A}$ is a symmetric positive definite matrix, defined as the MIL tensor.

From previous theoretical work given by Gibson (1985), and experimental work by Cater & Hayes (1977) and Bensusan et al. (1983), one observed that larger values of the MIL tensor $\boldsymbol{A}$ in a particular direction were associated with smaller values of Young's modulus of the equivalent homogeneous model. The fabric tensor $\boldsymbol{M}$ and the MIL tensor $\boldsymbol{A}$ was then related by Cowin (1986) as follows:

$$\boldsymbol{M} = \boldsymbol{A}^{-\frac{1}{2}} \tag{3}$$

The positive square root of the inverse of MIL tensor $\boldsymbol{A}$ is well-defined since it is a positive definite symmetric tensor that represents an ellipsoid (Cowin ,1986). The difference between MIL tensor and fabric tensor lies in the shape of the ellipsoid while the principal axes coincide.

From the spectral decomposition, the fabric tensor $\boldsymbol{M}$ can then be rewritten in terms of its eigenvalues m_i and eigenvectors $\boldsymbol{m}_i$ as follows:

$$\boldsymbol{M} = \sum_{i=1}^{3} m_i \boldsymbol{M}_i = \sum_{i=1}^{3} m_i (\boldsymbol{m}_i \otimes \boldsymbol{m}_i) \tag{4}$$

This matrix representation has many remarkable properties which make this method especially attractive. Specifically, finding the major material orientation involves finding the principal axes given by the eigenvectors of the fabric tensor (Harrigan & Mann, 1984). Furthermore, the degree of structural anisotropy is also quantified by the ratio between the maximum and minimum eigenvalues (Cowin, 1986).

3. RESULTS

In order to quantify the relevant morphological properties in porous anisotropic materials' behavior, the heterogeneous and orientation-dependent nature of these materials was taken into account by the porosity and the fabric tensor calculated by the Mean Intercept Length method. Some synthetic benchmark images were analyzed for better visualization of the method as a homogenization process. BoneJ plugin from ImageJ Software (Schneider et al., 2012) was used in this analysis. As the implemented algorithm takes random directions to construct MIL tensor, each case reported was run five times to establish the degree of anisotropy with 10^{-3} error order. All images have $120x122$ pixels resolution, and the configuration adopted for the MIL method was 3×10^3 directions and 1.5×10^4 lines per direction with 1.73 sampling increment. The fabric tensor was developed for each of the proposed cases, and the results are discussed.

3.1 Isotropic pattern

The isotropic case analysis started from a synthetic image constructed from equally spaced and symmetrically distributed circles in a defined square area. This pattern is shown in Figure 2.

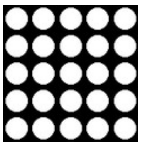

Figure 2. Benchmark isotropic image.

Anisotropy analysis via BoneJ for 2D cases generates the output shown in Table 1, where DA indicates the degree of anisotropy within a scale $[0,1]$; a and b represent, respectively, the minor and major radii of the semi-axes of the ellipse, calculated as previously presented by Eq. (3); $m00$, $m01$, $m10$, and $m11$ represent the components of the eigenvectors, listed as $m(row, column)$ in which each eigenvector is represented as a column; and $D1$ and $D2$ indicate the eigenvalues of the fabric tensor.

Table 1. Anisotropy analysis from BoneJ: isotropic pattern.

Porosity	DA	a	b	m00	m01	m10	m11	D1	D2
0.5167	0.0130	11.9617	12.0400	-0.0580	-0.9981	0.9983	-0.0580	0.0069	0.0070

a)

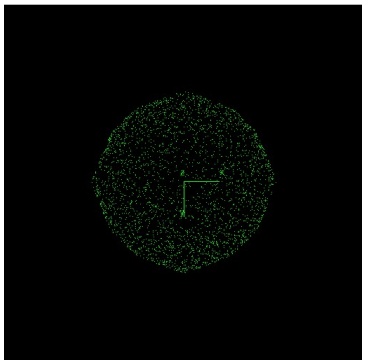

b)

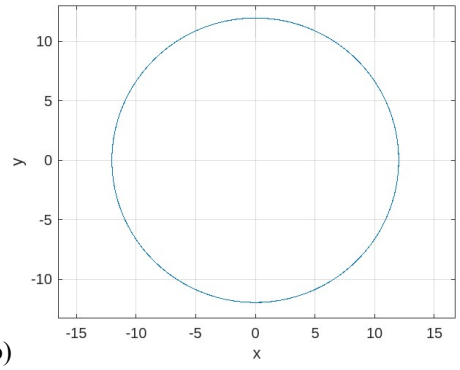

Figure 3. Isotropy pattern: a) MIL Point Vector (BoneJ); b) Ellipse created by fitting MIL data (MATLAB).

The MIL Point Vector cloud generated from the Anisotropy option in BoneJ is presented in Figure 3, as well as the quadratic curve that best fitted generated data in a post-processing stage in MATLAB. The generated results showed that the isotropic pattern was defined through approximately equal eigenvalues ($D1 = 0.0069$ and $D2 = 0.0070$) so that the fitted ellipse converges into a circle. In this case, the Degree of Anisotropy was calculated as 0.0130 or the equivalent of 1.3%, establishing a high level of isotropic condition.

3.2 Anisotropic patterns

For anisotropic cases, the analysis was performed from an oriented pattern image with different degrees of orientation, namely: 0°, 45°, 90°, and 135°. At this point, the aim was to analyze the relationship between orientation in simple patterns and the metrics given by the MIL tensor approach.

- Rotation 0°

  The oriented pattern at 0° rotation is shown in Figure 4.

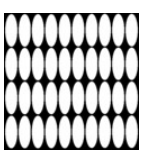

Figure 4. Benchmark anisotropic image (0°).

Anisotropy analysis in BoneJ generated the output shown in Table 2. The MIL Point Vector cloud and the ellipse that best fitted the generated data are presented in Figure 5.

Table 2. Anisotropy analysis from BoneJ: anisotropic pattern (0°).

Porosity	DA	a	b	m00	m01	m10	m11	D1	D2
0.6796	0.7726	6.3092	13.2293	0.9999	-0.0032	-0.0032	-0.9999	0.0057	0.0025

a) 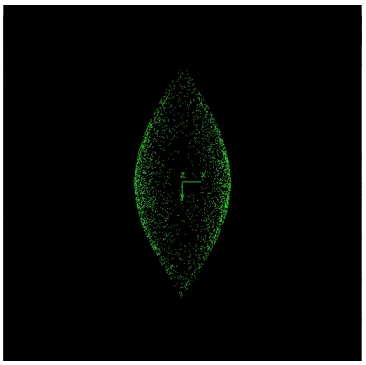 b) 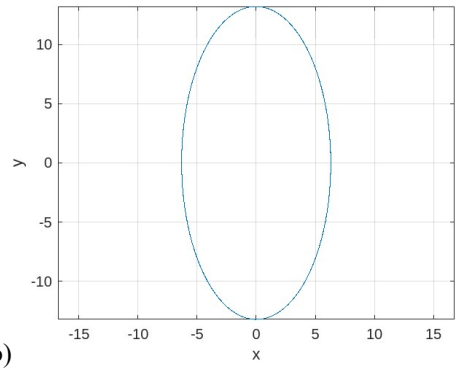

Figure 5. Anisotropy pattern (0°): a) MIL Point Vector (BoneJ); b) Ellipse created by fitting MIL data (MATLAB).

Based on the presented results, the MIL tensor indicates a predominantly vertical orientation and a degree of anisotropy equivalent to 77.26%. Due to the regularity of the analyzed pattern, the ellipse fitted from the MIL Point Vector cloud can be directly related to the orientation given by this anisotropic example.

- Rotation 45°

The oriented pattern at 45° rotation is shown in Figure 6.

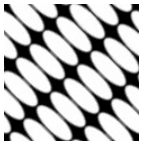

Figure 6. Benchmark anisotropic image (45°).

Anisotropy analysis generated the output shown in Table 3 and the MIL Point Vector cloud generated in BoneJ is presented in Figure 7, as well as the ellipse that best fitted the generated data.

Table 3. Anisotropy analysis from BoneJ: anisotropic pattern (45°).

Porosity	DA	a	b	m00	m01	m10	m11	D1	D2
0.6823	0.7725	8.4767	17.7708	0.7062	-0.7080	0.7080	0.7061	0.00317	0.0139

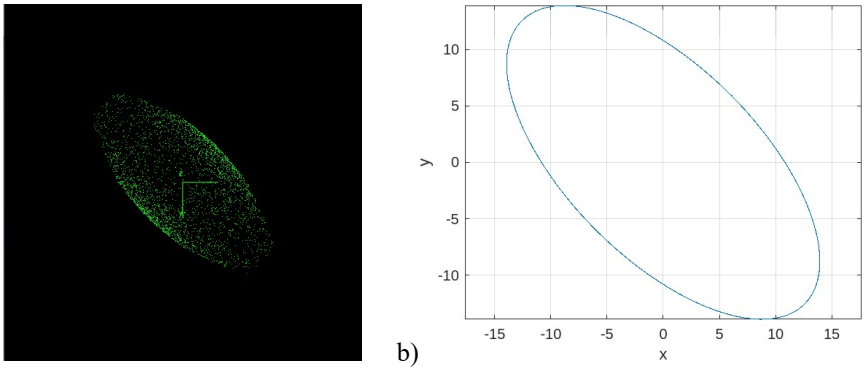

Figure 7. Anisotropy pattern (45°): a) MIL Point Vector (BoneJ); b) Ellipse created by fitting MIL data (MATLAB).

The generated results showed that the degree of anisotropy is equivalent to 77.25%, and the fitted ellipse is rotated by approximately 45.07°.

- Rotation 90°

The oriented pattern at 90° rotation is shown in Figure 8.

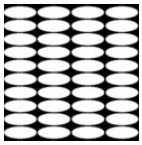

Figure 8. Benchmark anisotropic image (90°).

Anisotropy analysis generated the output shown in Table 4 and the MIL Point Vector cloud generated in BoneJ is presented in Figure 9, as well as the ellipse that best fitted the generated data.

Table 4. Anisotropy analysis from BoneJ: anisotropic pattern (90°).

Porosity	**DA**	**a**	**b**	**m00**	**m01**	**m10**	**m11**	**D1**	**D2**
0.6794	0.7888	6.2815	13.6689	0.0002	-0.9999	0.9999	0.0002	0.0054	0.0253

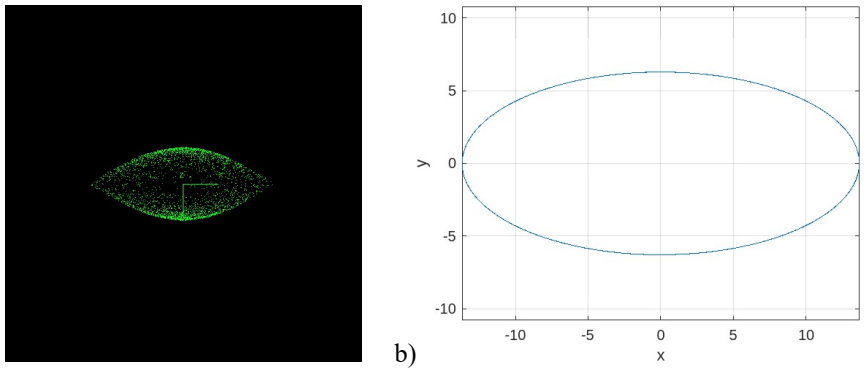

Figure 9. Anisotropy pattern (90°): a) MIL Point Vector (BoneJ); b) Ellipse created by fitting MIL data (MATLAB).

This analysis is comparable to the 0° rotation analysis, in which the horizontal axis similarly gives the main orientation. As for porosity, one can consider that there were no significant disagreements. For DA, a difference of approximately 2% was calculated. Regarding the eigenvalues, the difference was of the order of 10^{-4}. It should be reinforced that the MIL implemented algorithm is stochastic, so it is expected slight variations in the results, even when identical patterns are considered. Taking these aspects into account, the results were in good agreement with those expected.

- Rotation 135°

The oriented pattern at 135° rotation is shown in Figure 10.

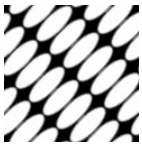

Figure 10. Benchmark anisotropic image (135°).

Anisotropy analysis generated the output shown in Table 5 and the MIL Point Vector cloud generated in BoneJ is presented in Figure 11, as well as the ellipse that best fitted the generated data.

Table 5. Anisotropy analysis from BoneJ: anisotropic pattern (135°).

Porosity	DA	a	b	m00	m01	m10	m11	D1	D2
0.6827	0.7763	8.4535	17.8687	-0.7067	-0.7075	0.7073	-0.7066	0.0031	0.0140

a) 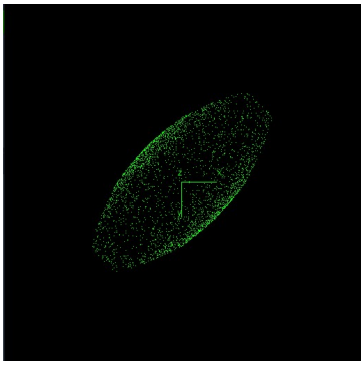 b) 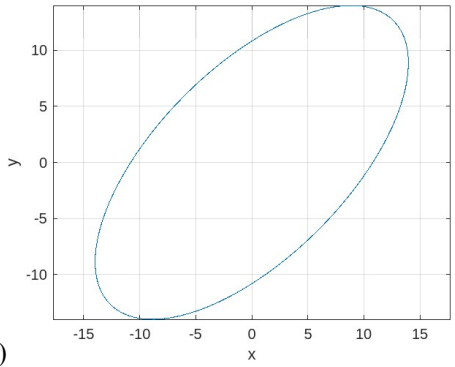

Figure 11. Anisotropy pattern (135°): a) MIL Point Vector (BoneJ); b) Ellipse created by fitting MIL data (MATLAB).

This analysis generated an anisotropy pattern similar to the 45° rotation pattern, which proves that the MIL tensor metrics calculated for these two cases must be equal. As for porosity, there were no significant disagreements. For DA, a difference of approximately 0.4% was calculated. Regarding the eigenvalues, the difference was of the order of 10^{-4}. The results were in good agreement with those expected.

3.3 Berea sandstone

An additional analysis was performed to evaluate the morphological properties for Berea Sandstone, a rock formation source of oil and gas, also known as Berea Grit. Imperial College London provided the dataset from the 3D Section of μ-CT image files. Figure 12.a) shows a cross-section of the μ-CT image of Berea Sandstone, and Figure 12.b) presents some of the slices considered during the analysis.

a) 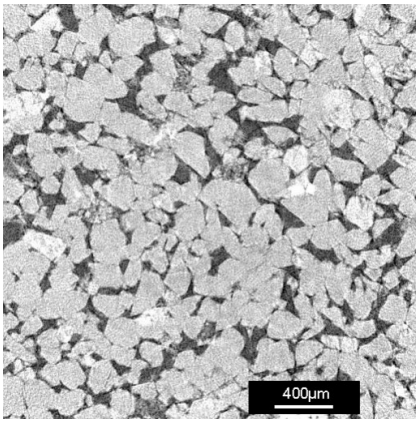

b) 

Figure 12. a) Cross-section of the µ-CT image of Berea Standstone; b) Binarized slices images of Berea Sandstone.

Anisotropy analysis output is shown in Table 6, and the MIL Point Vector cloud generated in BoneJ is presented in Figure 13, as well as the ellipsoid that best fitted the generated data.

Table 6. Anisotropy analysis from BoneJ: Berea Sandstone.

Porosity	DA	a	b	c	D1	D2	D3
0.1899	0.2436	22.6284	23.9457	26.0191	0.001476	0.001743	0.001952

m00	m01	m02	m10	m11	m12	m20	m21	m22
0.9396	0.2314	0.2519	0.2685	-0.0425	-0.9624	-0.2120	0.9719	-0.1020

a) 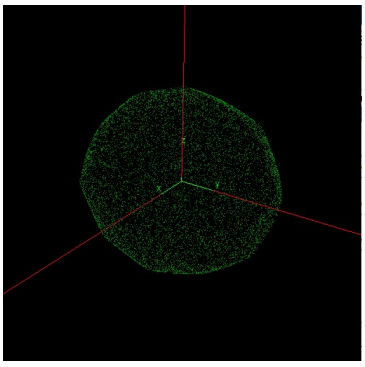
b) 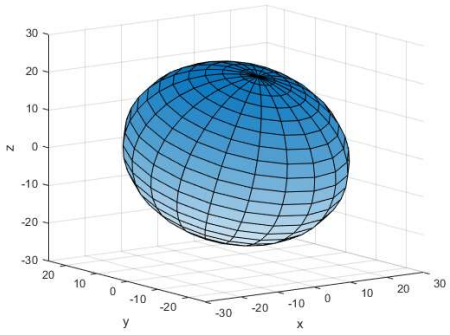

Figure 13: a) MIL Point (BoneJ); b) Ellipsoid created by fitting MIL data (MATLAB).

Concerning porosity, the results agree with the results calculated by Dong (2008) using this dataset. In this work, the author developed a maximal ball algorithm to extract topologically equivalent networks of pores and throats from images of porous media that can be used as input to network models. The porosity calculated from this method was 19%. In addition, the classic Berea network generated by Øren (2003) has a net porosity of 18.3%. Several works refer to anisotropy's influence on the material properties (Lo et al., 1986; Kim et al., 2016; Sato et al., 2018). However, to the best of the author's knowledge, there are no records of quantifying the anisotropy in terms of fabric tensors.

4. CONCLUSIONS

Although volume fraction (or porosity) is considered the primary parameter in the geometric characterization of the microstructure of porous materials, it does not provide any information about the arrangement of the microstructure. In this regard, the approach used to model the microstructure architecture involves introducing higher-ranking fabric tensors. Among the methods proposed in the literature, the Mean Intercept Length (MIL) method is investigated, and its fabric tensor construction ability and characteristics were analyzed through simple examples.

Synthetic benchmark images were analyzed for better visualization of the method as a homogenization process. In each of the cases, the porosity, the fabric tensor, and the degree of anisotropy were calculated using BoneJ plugin from ImageJ Software. Initially, an isotropic pattern image constructed from equally spaced and symmetrically distributed circles in a defined square area was analyzed. The results showed approximately equal eigenvalues so that the fitted ellipse converges into a circle. The Degree of Anisotropy was calculated as 0.0130 or the equivalent of 1.3%, establishing a high level of isotropic condition. Next, anisotropic cases were performed from an oriented pattern image with same porosity but different degrees of orientation, namely: 0°, 45°, 90°, and 135°. From anisotropic pattern (0°) analysis, the MIL tensor indicated a predominantly vertical orientation and a degree of anisotropy equivalent to 77.26%. Moreover, the ellipse fitted from the MIL Point Vector cloud could be directly related to the orientation given by this anisotropic example. This analysis was also compared to the anisotropic pattern (90°) case, since both present similar patterns of anisotropy in which the main direction is given by the vertical and the horizontal axis, respectively. As for porosity, there were no significant disagreements. For DA, a difference of approximately 2% was calculated. Regarding the eigenvalues, the difference was of the order of 10^{-4}. Similarly, the anisotropic pattern (45°) analysis was compared to the results provided by the anisotropic pattern (135°) case. As for porosity, again there were no significant disagreements. For DA, a difference of approximately 0.4% was calculated and regarding the eigenvalues, the difference was of the order of 10^{-4}.

It must be highlighted that the MIL implemented algorithm is stochastic so that slight variations in the results are expected, even when identical patterns are considered. An additional case was performed to consider the morphological properties from μ-CT image analysis of Berea Sandstone. The calculated porosity was 18,99% and considered in good agreement to previously published results. The ellipsoid that best fitted the generated data was also defined in terms of fabric tensor eigenvalues and eigenvectors, which open the perspective of using this tool to incorporate this morphological parameter in elasticity models and failure criteria for anisotropic porous materials.

5. REFERENCES

Badakhshan, E., Noorzad, A., Bouazza, A., and Xu, C. (2021). Application of particle stiffness fabric tensor for modeling inherent anisotropy in rocks. Rock Mechanics and Rock Engineering, 54(6):3077–3093.

Bensusan, J., Davy, D., Heiple, K., and Verdin, P. (1983). Tensile, compressive and torsional testing of cancellous bone. Trans Orthop Res Soc, 8:132.

Cater, D. R. and Hayes, W. C. (1977). The compressive behavior of bone as a two-phase porous structure. Journal of Bone Joint Surgery, 59:954–962.

Chakrabarty, J. (2012). Theory of plasticity. Elsevier.

Charlebois, M., Pretterklieber, M., and Zysset, P. K. (2010). The role of fabric in the large strain compressive behavior of human trabecular bone. Journal of Biomechanical Engineering, 132(12).

Chiang, M. Y., Wang, X., Landis, F. A., Dunkers, J., and Snyder, C. R. (2006). Quantifying the directional parameter of structural anisotropy in porous media. Tissue engineering, 12(6):1597–1606.

Cowin, S. C. (1985). The relationship between the elasticity tensor and the fabric tensor. Mechanics of materials, 4(2), 137-147.

Cowin, S. C. (1986). Wolff's law of trabecular architecture at remodeling equilibrium.

De Pascalis, F., Lionetto, F., Maffezzoli, A., and Nacucchi, M. (2022). A general approach to calculate the stiffness tensor of short-fiber composites using the fabric tensor determined by x-ray computed tomography. Polymer Composites.

Dong, H. (2008). Micro-CT imaging and pore network extraction. Ph.D. thesis, Department of Earth Science and Engineering, Imperial College London.

Gao, Z., Zhao, J., and Yao, Y. (2010). A generalized anisotropic failure criterion for geomaterials. International Journal of Solids and Structures, 47(22-23):3166–3185.

Gibson, L. (1985). The mechanical behaviour of cancellous bone. Journal of Biomechanics, 18(5):317–328.

Harrigan, T. P. and Mann, R. W. (1984). Characterization of microstructural anisotropy in orthotropic materials using a second rank tensor. J. Mater. Sci., 19(3):761–767.

Hill, R. (1998). The mathematical theory of plasticity, Vol. 11. Oxford University Press.

Hu, N., Zhuang, P.-Z., Yang, D.-S., and Yu, H.-S. (2021). On the evolution law of a contact normal-based fabric tensor for granular materials. Computers and Geotechnics, 132:103857.

Jeppesen, N., Mikkelsen, L., Dahl, A., Christensen, A., and Dahl, V. (2021). Quantifying effects of manufacturing methods on fiber orientation in unidirectional composites using structure tensor analysis. Composites Part A: Applied Science and Manufacturing, 149:106541.

Kahl, W.A., Dilissen, N., Hidas, K., Garrido, C. J., López-Sanchez, V., and Alpiste, R. (2017). 3-D Microstructure of olivine in complex geological materials reconstructed by correlative X-Ray-CT and EBSD analyses. Journal of Microscopy, 268(2):193–207.

Keralavarma, S. and Chockalingam, S. (2016). A criterion for void coalescence in anisotropic ductile materials. International Journal of Plasticity, 82:159–176.

Ketcham, R. A. (2005). Three-dimensional grain fabric measurements using high-resolution X-ray computed tomography. Journal of Structural Geology, 27(7):1217–1228.

Kim, K. Y., Zhuang, L., Yang, H., Kim, H., and Min, K.-B. (2016). Strength anisotropy of Berea sandstone: results of x-ray computed tomography, compression tests, and discrete modeling. Rock Mechanics and Rock Engineering, 49:1201–1210.

Kreipke, T. and Niebur, G. (2017). Anisotropic permeability of trabecular bone and its relationship to fabric and architecture: a computational study. Annals of Biomedical Engineering, 45(6):1543–1554.

Lekadir, K., Noble, C., Hazrati-Marangalou, J., Hoogendoorn, C., van Riet-Bergen, B., Taylor, Z. A., and Frangi, A. F. (2016). Patient-specific biomechanical modeling of bone strength using statistically derived fabric tensors. Annals of biomedical engineering, 44(1):234–246.

Lo, T., Coyner, K., and Toksöz, M. (1986). Experimental determination of elastic anisotropy of Berea sandstone, chicopee shale, and chelmsford granite: Geophysics.

Lydzba, D., Pietruszczak, S., and Shao, J.-F. (2003). On anisotropy of stratified rocks: homogenization and fabric tensor approach. Computers and Geotechnics, 30(4):289–302.

Moreno, R., Borga, M., and Smedby, O. (2014). Techniques for computing fabric tensors: A review, pages 271–292.

Moreno, R., Smedby, Ö., and Borga, M. (2011). On the efficiency of the mean intercept length tensor.

Moreno, R., Smedby, Ö., and Pahr, D. H. (2016). Prediction of apparent trabecular bone stiffness through fourth-order fabric tensors. Biomechanics and modeling in mechanobiology, 15(4):831–844.

Øren, P.-E. and Bakke, S. (2003). Reconstruction of Berea sandstone and pore-scale modeling of wettability effects. Journal of Petroleum Science and Engineering, 39(3-4):177–199.

Pietruszczak, S. and Mroz, Z. (2001). On failure criteria for anisotropic cohesive-frictional materials. International Journal for Numerical and Analytical Methods in Geomechanics, 25(5):509–524. Hosford, W. F. (2010). Mechanical Behavior of Materials. Cambridge University Press.

Pietruszczak, S. and Pakdel, P. (2022). On the mechanical anisotropy of argillaceous Cobourg limestone: fabric tensor approach. International Journal of Rock Mechanics and Mining Sciences, 150:104953.

Sadd, M. H. (2018). Continuum mechanics modeling of material behavior. Academic Press.

Sato, M., Takemura, T., and Takahashi, M. (2018). Development of the permeability anisotropy of submarine sedimentary rocks under true triaxial stresses. International Journal of rock mechanics and mining sciences, 108:118–127.

Schneider, C. A., Rasband, W. S., & Eliceiri, K. W. (2012). NIH Image to ImageJ: 25 years of image analysis. Nature Methods, 9(7), 671–675.

Singh, A. K., Srivastava, P., Kumar, N., and Mahajan, P. (2022). A fabric tensor based small strain constitutive law for the elastoplastic behavior of snow. Mechanics of Materials, 165:104182.

Skrzypek, J. J., & Ganczarski, A. W. (Eds.). (2015). Mechanics of Anisotropic Materials (pp. 57-86). Cham, Switzerland: Springer International Publishing.

Smolin, A. Y., Eremina, G., and Korostelev, S. Y. (2019). Methods for describing structure of novel porous materials: a review. In IOP Conference Series: Materials Science and Engineering, Vol. 696, page 012017. IOP Publishing.

Underwood, E. E. (1973). Quantitative stereology for microstructural analysis.

Voyiadjis, G. Z. and Kattan, P. I. (1999). Advances in Damage Mechanics: Metals and Metal Matrix Composites. Elsevier.

Voyiadjis, G. Z., Kattan, P. I., and Taqieddin, Z. N. (2007). Continuum approach to damage mechanics of composite materials with fabric tensors. International Journal of Damage Mechanics, 16(3):301–329.

Whitehouse, W. J. (1974). The quantitative morphology of anisotropic trabecular bone. Journal of Microscopy, 101(2):153–168.

6. RESPONSIBILITY NOTICE

The authors are the only ones responsible for the printed material included in this paper.